

# ISTA-Inspired Network for Image Super-Resolution

Yuqing Liu<sup>1</sup>, Wei Zhang<sup>1,\*</sup>, Weifeng Sun<sup>2</sup>, Zhikai Yu<sup>1</sup>, Jianfeng Wei<sup>1</sup> and Shengquan Li<sup>1</sup>

<sup>1</sup> Pengcheng Laboratory, Shenzhen, China.

<sup>2</sup> Dalian University of Technology, Dalian, China.

**Abstract**—Deep learning for image super-resolution (SR) has been investigated by numerous researchers in recent years. Most of the works concentrate on effective block designs and improve the network representation but lack interpretation. There are also iterative optimization-inspired networks for image SR, which take the solution step as a whole without giving an explicit optimization step. This paper proposes an unfolding iterative shrinkage thresholding algorithm (ISTA) inspired network for interpretable image SR. Specifically, we analyze the problem of image SR and propose a solution based on the ISTA method. Inspired by the mathematical analysis, the ISTA block is developed to conduct the optimization in an end-to-end manner. To make the exploration more effective, a multi-scale exploitation block and multi-scale attention mechanism are devised to build the ISTA block. Experimental results show the proposed ISTA-inspired restoration network (ISTAR) achieves competitive or better performances than other optimization-inspired works with fewer parameters and lower computation complexity.

## I. INTRODUCTION

Image super-resolution (SR), as one of the traditional image restoration tasks, has been widely investigated by researchers [1], [2]. Given a low-resolution (LR) image, the task of image SR is to restore a corresponding high-resolution (HR) instance with more details. There are numerous applications considering the image SR, such as video deinterlacing [3] and compression [4], remote sensing [5]–[7], EGG analysis [8], and spatio-spectral analysis [9].

Deep learning has demonstrated its amazing performance in image restoration. There are numerous convolutional neural networks (CNNs) specially designed for image SR. SRCNN [10] is the first CNN-based method for image SR. After that, deeper and wider networks show their effectiveness with better performance, such as VDSR [11], EDSR [12], RDN [13] and RCAN [14]. Recent image SR networks usually develop effective blocks for improving the network representation. IMDN [15] and EFDN [16] utilize information distillation mechanisms to build an efficient network for fast and accurate image SR. Cross-SRN [17] builds an edge-preserving network with cross convolution. However, these works concentrate on the block designs but lack interpretation, which limits the performance.

Since image SR can be regarded as a classical optimization task [18], there are also works considering building the image SR network from the optimization perspective. IRCNN [18] provides an iterative solution for the general image restoration task and designs a CNN-based network to solve the denoising prior. ISRN [19] develops an iterative network with the help of the half-quadratic splitting (HQS) strategy. DPSR [20] and USRNet [21] also achieve good performance on image SR

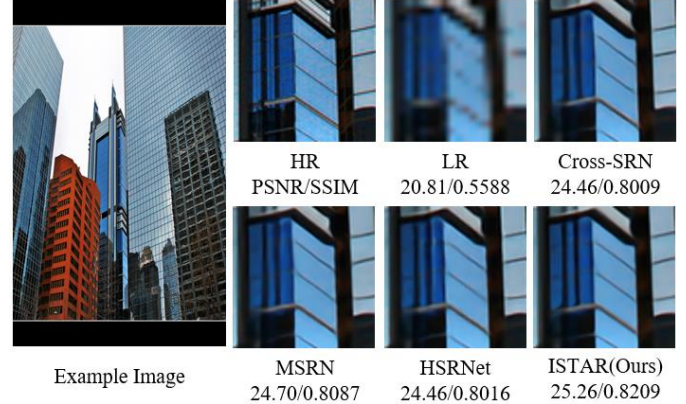


Fig. 1. An example comparison among different image super-resolution methods.

inspired by the HQS strategy. There are also works building the network by alternating direction method of multipliers (ADMM). Plug-and-Play ADMM [22] regards the denoiser as a network prior for different image restoration tasks. ADMM-Net [23] provides an end-to-end network for the compression sensing task. PSRI-Net [24] considers ADMM for SAR image SR. Although these works provide an interpretable network design, the CNN architectures just task the solution step as a whole, without giving an explicit optimization step on how to solve the denoising problem.

In this paper, we develop an unfolding network based on the iterative shrinkage thresholding algorithm (ISTA). Different from designing the CNN to directly solve the optimization step, ISTA blocks are specially designed to conduct the image restoration following the ISTA steps. In the ISTA block, CNNs are utilized to adaptively learn the functions in the feature space and speed up the optimization steps. To improve the network representation, multi-scale exploration (MSE) and multi-scale attention (MSA) mechanisms are utilized to build the ISTA block. An ISTA-inspired restoration network (ISTAR) is developed based on the ISTA block for effective image SR. Experimental results show the proposed ISTAR can achieve competitive or better performance than other works. Compared with other optimization-inspired methods, ISTAR achieves better performances with much fewer parameters and lower computation complexity. Figure 1 shows an example comparison among different image super-resolution methods. Compared with state-of-the-art methods, our proposed ISTAR can generate more satisfying textures that close to the HR image.

The contributions of this paper can be concluded as follows:

- We analyze the image super-resolution task from the optimization perspective and develop an ISTA block for image super-resolution.
- We develop the multi-scale exploration and multi-scale attention mechanism in the ISTA block, which improves the network representation and boosts the performance.
- Experimental results show the proposed network achieves competitive or better performance than other optimization-based works with much fewer parameters and lower computation complexity.

## II. RELATED WORKS

### A. Deep Learning for Image Super-Resolution

Deep learning has demonstrated its amazing performance on various computer vision tasks. There are numerous convolutional neural networks (CNNs) specially designed for image super-resolution (SR). SRCNN [10] is the first CNN-based image SR method composed of three convolution layers, which follows a sparse-coding manner. After SRCNN, deeper and wider networks has proposed to improve the restoration performance. FSRCNN [25] increases the network depth and decreases the input resolution, which makes the method faster and more effective. VDSR [11] develops a very deep network with residual connection to restore the high-resolution (HR) images. EDSR [12] then utilizes the residual blocks in the network and improves the network capacity. ESPCN [26] provides a different upsampling strategy to restore the HR images, which is more effective than the deconvolution operation. Recently, researchers concentrate more on effective block design for better restoration performance. RDN [13] combines the residual connection [27] and densely connection [28], and develops a residual dense block for image SR. After that, the researchers introduce the residual-in-residual design with channel attention [29] for image SR and build an effective network termed RCAN [14]. RFANet [30] expands the residual connection and aggregates the residual features for better information transmission. IMDN [15] and RFDN [16] build the lightweight networks with the help of an information distillation mechanism. SHSR [31] and MSRN [32] utilize hierarchical exploration to further investigate the image features. These works usually concentrate on the effective block designs but neglect to analyze the image SR from the optimization perspective.

### B. Optimization-Inspired Image Super-Resolution

There are also optimization-inspired networks for interpretable image SR. ADMM-Net [23] provides a good example of dealing with the image restoration problem by the optimization strategy and develops a CNN-based denoiser for plug-and-play restoration. IRCNN [18] then analyzes the image restoration with the help of the half-quadratic splitting (HQS) strategy and recovers the image with a CNN-based denoiser prior. After IRCNN, there are numerous HQS-based methods for effective image SR. DPSR [20] proposes a different observation model for image SR and uses kernel estimation and CNN denoiser for plug-and-play image SR. USRNet [21] develops an end-to-end network for different image SR tasks.

ISRN [19] devises an effective network for image SR under the guidance of HQS and maximum likelihood estimation (MLE). HSRNet [33] also investigates the HQS strategy and develops a network for aliasing suppression image SR. However, these works just take the solution as a whole and calculate it directly by CNNs, without giving an explicit optimization step for each iteration.

## III. METHODOLOGY

In this section, we first analyze the image super-resolution (SR) from the optimization perspective and propose an iterative solution with the help of ISTA. Then, we introduce the designed end-to-end network ISTAR. After that, we discuss the design of the ISTA block. Finally, the network settings are described in detail.

### A. ISTA for Image Super-Resolution

Given an low-resolution (LR) image  $I^{LR}$ , the task of image SR is to find a corresponding image  $I^{SR}$ , satisfying

$$I^{SR} = \arg \min_{I^{SR}} \|DI^{SR} - I^{LR}\|_{\ell}^2 + \lambda \|I^{LR}\|_1, \quad (1)$$

where  $D$  is the down-sampling matrix, and  $\lambda$  is a weighting factor. The prior term  $\lambda \|I^{LR}\|_1$  is utilized to introduce the sparsity of the natural image.

To solve this function, we use ISTA to convert it into an iterative manner. Then, the solution is

$$I_{k+1}^{SR} = \mathcal{T}_{\lambda\alpha_k}(I_k^{SR} - \alpha_k D^T (DI_k^{SR} - I^{LR})), \quad (2)$$

where  $\alpha_k$  is the weighting factor for the  $k$ -th iteration and  $\mathcal{T}(\cdot)$  is the soft-thresholding operation.

It can be found that the right hand side of Equation 2 has two independent variables  $I_k^{SR}$  and  $I^{LR}$ . To make it clear for understanding, we re-write Equation 2 as

$$I_{k+1}^{SR} = \mathcal{T}_{\lambda\alpha_k}((E - \alpha_k D^T D)I_k^{SR} - \alpha_k D^T I^{LR}), \quad (3)$$

where  $E$  is the identity matrix.

In Equation 3, we can find that  $D^T I^{LR}$  is shared for every iteration. In this point of view, we can calculate this term before the ISTA optimization, and regard it as an invariant to speed up the optimization.

### B. Network Design

Figure 2 shows the entire network design of our ISTAR. Firstly, the input image  $I^{LR}$  is converted into the feature space by one convolutional layer as

$$\hat{I}^{LR} = Conv(I^{LR}). \quad (4)$$

Then, two convolutional layers and one ReLU activation are utilized to calculate the  $D^T I^{LR}$  for ISTA steps, as shown in the figure. There are  $K$  steps for ISTA optimization. For the  $k$ -th step, there is

$$\hat{I}_k^{SR} = ISTABlock(D^T I^{LR}, \hat{I}_{k-1}^{SR}), \quad (5)$$

where  $ISTABlock(\cdot)$  is the designed ISTA block.

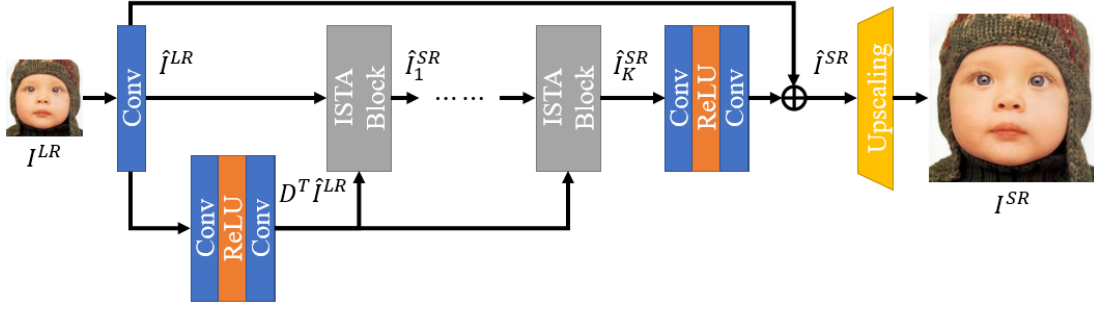


Fig. 2. Network design of ISTAR

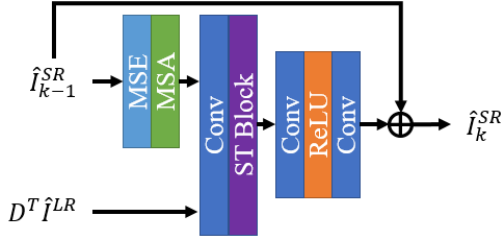


Fig. 3. ISTA Block design

After  $K$  iterations, the output  $\hat{I}_K^{SR}$  and  $\hat{I}^{LR}$  are organized in a skip connection manner as

$$\hat{I}^{SR} = \hat{I}^{LR} + \text{Padding}(\hat{I}_K^{SR}), \quad (6)$$

where  $\text{Padding}(\cdot)$  aims to introduce the non-linearity. The padding structure is composed of two convolutional layers and one ReLU activation. Finally, the restored image  $I^{SR}$  is generated from the SR feature  $\hat{I}^{SR}$  as

$$I^{SR} = \text{Upscaling}(\hat{I}^{SR}), \quad (7)$$

where  $\text{Upscaling}(\cdot)$  is the upscaling module. The upscaling module is composed of one convolutional layer and a sub-pixel convolution.

### C. Design of ISTA Block

Figure 3 shows the ISTA block design. The inputs of  $k$ -th ISTA block are  $\hat{I}_{k-1}^{SR}$  and  $D^T I^{LR}$ , and the output of the block is  $\hat{I}_k^{SR}$ . Multi-scale exploration (MSE) block and multi-scale attention (MSA) mechanism are utilized to generate  $(E - \alpha_k D^T D)\hat{I}_k^{SR}$  from  $\hat{I}$ . Then, one  $1 \times 1$  convolution combines the information from the  $(E - \alpha_k D^T D)\hat{I}_k^{SR}$  and the  $D^T I^{LR}$ , and the soft-thresholding block (ST Block) jointly explores the features following the Equation 3. A padding structure is introduced to the ISTA block with skip connection for better gradient transmission. The padding structure is composed of two convolutional layers and a ReLU activation.

Figure 4 shows the block design of MSE. Multi-scale design has proved to be an effective structure for image SR. In this block, three different scales ( $1 \times 1$ ,  $3 \times 3$ , and  $5 \times 5$ ) are considered to explore the hierarchical information from the features. To make the exploration more efficient, the  $5 \times 5$  exploration is separated into two  $3 \times 3$  convolutions with a ReLU activation, which hold the same receptive field. After

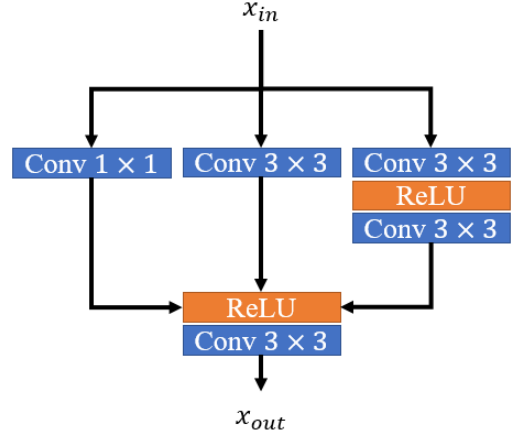


Fig. 4. Multi-scale exploration (MSE) block design

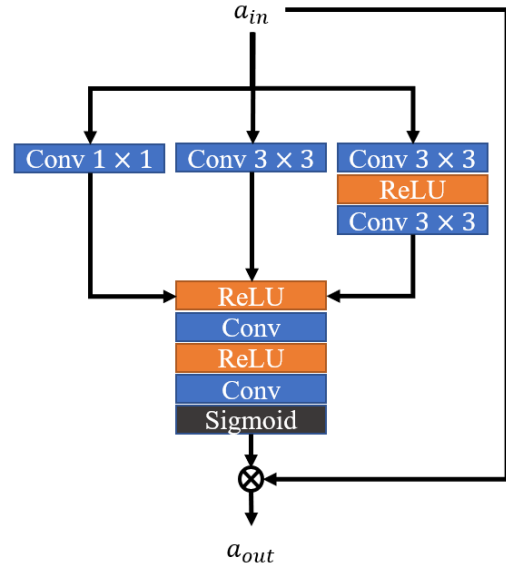


Fig. 5. Multi-scale attention (MSA) mechanism design

the multi-scale feature extraction, one ReLU activation and a convolutional layer concatenate the hierarchical features and generate the final output of the MSE.

Figure 5 shows the block design of multi-scale attention (MSA) mechanism. It can be found that the MSA has a similar multi-scale exploration design as MSE. Hierarchical

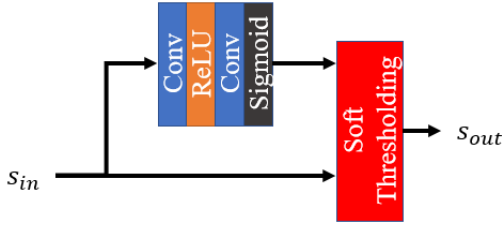


Fig. 6. Soft thresholding block (ST Block) design

TABLE I  
PSNR/SSIM COMPARISONS AMONG DIFFERENT ITERATION TIMES WITH SCALING FACTOR  $\times 4$ .

$K$	Set14	B100	Urban100	Manga109
4	28.46/0.7786	27.47/0.7330	25.75/0.7748	30.06/0.9020
8	28.50/0.7810	27.53/0.7352	25.95/0.7827	30.33/0.9063
12	28.57/0.7809	27.57/0.7352	26.04/0.7842	30.46/0.9074
16	28.59/0.7822	27.59/0.7372	26.11/0.7886	30.54/0.9089

features from three different scales are jointly explored by two convolutional layers and two ReLU activation operations. Then, the Sigmoid activation is introduced to generate the non-negative attention information.

Figure 6 shows the soft-thresholding block (ST Block) design. The ST Block is composed of two  $1 \times 1$  convolutional layers, one ReLU activation and a Sigmoid activation. The ST Block calculates the hyper parameters from the input features by the network design, and performs the soft-thresholding action with the learned parameters.

#### D. Network Details

In the network, all convolution kernels are set with size  $3 \times 3$  except for the MSE and the ST Block. The convolutions in ST Block are set with kernel size as  $1 \times 1$ . The filters of all convolutional layers are set with 64 except for the ST Block and the Upscaling module. There are  $K = 16$  ISTA blocks in the ISTAR. The loss function is chosen as  $\ell_1$ -norm between the SR and HR images.

## IV. EXPERIMENT

### A. Settings

The network is trained with DIV2K [34] dataset, which contains 900 high resolution images. We choose first 800 images for training, and last 5 image for validation. Five common benchmarks are chosen for comparing the restoration effectiveness: Set5 [35], Set14 [36], B100 [37], Urban100 [38] and Manga109 [39]. We update our ISTAR for 1000 epochs by the Adam [40] optimizer with learning rate  $10^{-4}$ . The learning rate is halved for every 200 epochs. The scaling factors are chosen as  $\times 2$ ,  $\times 3$  and  $\times 4$ . The patch size for training is chosen as  $48 \times 48$  for LR images. All other settings are same as RDN [13]. The objective indicators are chosen as peak signal-to-noise ratio [41] (PSNR) and structural similarity [42] (SSIM).

TABLE II  
PSNR/SSIM COMPARISONS AMONG MULTI-SCALE EXPLORATIONS WITH SCALING FACTOR  $\times 4$ .

$S$	B100	Urban100	Manga109
1	27.55/0.7354	26.00/0.7835	30.40/0.9067
(1 + 3)	27.55/0.7355	26.03/0.7844	30.49/0.9073
(1 + 3 + 5)	27.59/0.7372	26.11/0.7886	30.54/0.9089

TABLE III  
PSNR/SSIM COMPARISONS BETWEEN MSA WITH SCALING FACTOR  $\times 4$ .

MSA	Set14	B100	Urban100	Manga109
w/o	28.67/0.7874	27.64/0.7388	26.32/0.7942	30.77/0.9120
w	28.74/0.7855	27.66/0.7391	26.38/0.7955	30.87/0.9130

### B. Model Analysis

1) *Investigation on the Iteration Times:* According to the ISTA optimization, the result becomes more accurate with the increase of iteration times. To investigate the effectiveness of the iteration times, we compare the performances with different iteration time  $K$ . Table I shows the PSNR/SSIM comparisons among different  $K$  with scaling factor  $\times 4$ . For a fair comparison, all the testing models are updated for 200 epochs under the same settings. In the table, we can find that the PSNR and SSIM rises with the increase of iteration time  $K$ . When  $K = 16$ , the network achieves the best performance. In this point of view, a deeper network leads to a better performance. When  $K$  increases from 12 to 16, the PSNR and SSIM gets small improvement. To balance the performance and the computation complexity, we choose  $K = 16$  to build the ISTAR.

2) *Investigation on the Multi-Scale Exploration:* In MSE, we utilize three different scales to explore the hierarchical information. To investigate the effectiveness of multi-scale exploration, we conduct the experiments with scaling combination as 1, (1 + 3) and (1 + 3 + 5). Table II shows the PSNR/SSIM comparisons among different scales combinations. In the figure, we can find that the multi-scale exploration brings 0.08 dB PSNR improvement on Urban100 dataset and 0.05 db improvement on Manga109 dataset. Compared with  $S = 1$ , the combination (1 + 3) brings 0.09 dB PSNR improvement on Manga109 dataset. In this point of view, the multi-scale exploration is an effective design for restoration.

3) *Investigation on the Multi-Scale Attention:* In ISTA block, MSA is considered for better network representation. To show the effectiveness of MSA, we compare the objective performances with and without MSA on different benchmarks. Table III shows the PSNR/SSIM comparisons after training 1000 epochs. In the figure, we can find that the network with MSA has 0.1 dB improvement on Manga109 dataset and 0.06 dB improvement on Set14 and Urban100 dataset. In this point of view, the MSA proves to be an effective component for image restoration and improves the network capacity.

### C. Results

We compare our ISTAR with several traditional and recent CNN-based image SR works: SRCNN [10], FSR-CNN [25], VDSR [11], DRCN [43], CNF [44], LapSRN [45],

TABLE IV  
PSNR/SSIM COMPARISONS WITH SCALING FACTOR  $\times 2$ ,  $\times 3$ , AND  $\times 4$  ON FIVE BENCHMARKS. THE BEST PERFORMANCES ARE SHOWN IN **BOLD**.

Scale	Model	Set5 [35] PSNR/SSIM	Set14 [36] PSNR/SSIM	B100 [37] PSNR/SSIM	Urban100 [38] PSNR/SSIM	Manga109 [39] PSNR/SSIM
$\times 2$	SRCNN [10]	36.66 / 0.9542	32.42 / 0.9063	31.36 / 0.8879	29.50 / 0.8946	35.74 / 0.9661
	FSRCNN [25]	37.00 / 0.9558	32.63 / 0.9088	31.53 / 0.8920	29.88 / 0.9020	36.67 / 0.9694
	VDSR [11]	37.53 / 0.9587	33.03 / 0.9124	31.90 / 0.8960	30.76 / 0.9140	37.22 / 0.9729
	DRCN [43]	37.63 / 0.9588	33.04 / 0.9118	31.85 / 0.8942	30.75 / 0.9133	37.63 / 0.9723
	CNF [44]	37.66 / 0.9590	33.38 / 0.9136	31.91 / 0.8962	-	-
	LapSRN [45]	37.52 / 0.9590	33.08 / 0.9130	31.80 / 0.8950	30.41 / 0.9100	37.27 / 0.9740
	DRRN [46]	37.74 / 0.9591	33.23 / 0.9136	32.05 / 0.8973	31.23 / 0.9188	37.92 / 0.9760
	BTSRN [47]	37.75 / -	33.20 / -	32.05 / -	31.63 / -	-
	MemNet [48]	37.78 / 0.9597	33.28 / 0.9142	32.08 / 0.8978	31.31 / 0.9195	37.72 / 0.9740
	SelNet [49]	37.89 / 0.9598	33.61 / 0.9160	32.08 / 0.8984	-	-
	CARN [50]	37.76 / 0.9590	33.52 / 0.9166	32.09 / 0.8978	31.92 / 0.9256	38.36 / 0.9765
	IMDN [15]	38.00 / 0.9605	33.63 / 0.9177	32.19 / 0.8996	32.17 / 0.9283	38.88 / 0.9774
	RAN [51]	37.58 / 0.9592	33.10 / 0.9133	31.92 / 0.8963	-	-
	DNCL [52]	37.65 / 0.9599	33.18 / 0.9141	31.97 / 0.8971	30.89 / 0.9158	-
	FilterNet [53]	37.86 / 0.9610	33.34 / 0.9150	32.09 / 0.8990	31.24 / 0.9200	-
	MRFN [54]	37.98 / 0.9611	33.41 / 0.9159	32.14 / 0.8997	31.45 / 0.9221	38.29 / 0.9759
	SeaNet-baseline [55]	37.99 / 0.9607	33.60 / 0.9174	32.18 / 0.8995	32.08 / 0.9276	38.48 / 0.9768
	DEGREE [56]	37.58 / 0.9587	33.06 / 0.9123	31.80 / 0.8974	-	-
Cross-SRN [57]	38.03 / 0.9606	33.62 / 0.9180	32.19 / 0.8997	32.28 / 0.9290	38.75 / 0.9773	
ISTAR (Ours)	<b>38.15 / 0.9610</b>	<b>33.79 / 0.9197</b>	<b>32.29 / 0.9010</b>	<b>32.65 / 0.9331</b>	<b>38.96 / 0.9777</b>	
$\times 3$	SRCNN [10]	32.75 / 0.9090	29.28 / 0.8209	28.41 / 0.7863	26.24 / 0.7989	30.59 / 0.9107
	FSRCNN [25]	33.16 / 0.9140	29.43 / 0.8242	28.53 / 0.7910	26.43 / 0.8080	30.98 / 0.9212
	VDSR [11]	33.66 / 0.9213	29.77 / 0.8314	28.82 / 0.7976	27.14 / 0.8279	32.01 / 0.9310
	DRCN [43]	33.82 / 0.9226	29.76 / 0.8311	28.80 / 0.7963	27.15 / 0.8276	32.31 / 0.9328
	CNF [44]	33.74 / 0.9226	29.90 / 0.8322	28.82 / 0.7980	-	-
	DRRN [46]	34.03 / 0.9244	29.96 / 0.8349	28.95 / 0.8004	27.53 / 0.8378	32.74 / 0.9390
	BTSRN [47]	34.03 / -	29.90 / -	28.97 / -	27.75 / -	-
	MemNet [48]	34.09 / 0.9248	30.00 / 0.8350	28.96 / 0.8001	27.56 / 0.8376	32.51 / 0.9369
	SelNet [49]	34.27 / 0.9257	30.30 / 0.8399	28.97 / 0.8025	-	-
	CARN [50]	34.29 / 0.9255	30.29 / 0.8407	29.06 / 0.8034	28.06 / 0.8493	33.50 / 0.9440
	IMDN [15]	34.36 / 0.9270	30.32 / 0.8417	29.09 / 0.8046	28.17 / 0.8519	33.61 / 0.9445
	RAN [51]	33.71 / 0.9223	29.84 / 0.8326	28.84 / 0.7981	-	-
	DNCL [52]	33.95 / 0.9232	29.93 / 0.8340	28.91 / 0.7995	27.27 / 0.8326	-
	FilterNet [53]	34.08 / 0.9250	30.03 / 0.8370	28.95 / 0.8030	27.55 / 0.8380	-
	MRFN [54]	34.21 / 0.9267	30.03 / 0.8363	28.99 / 0.8029	27.53 / 0.8389	32.82 / 0.9396
	SeaNet-baseline [55]	34.36 / 0.9280	30.34 / 0.8428	29.09 / 0.8053	28.17 / 0.8527	33.40 / 0.9444
	DEGREE [56]	33.76 / 0.9211	29.82 / 0.8326	28.74 / 0.7950	-	-
	Cross-SRN [57]	34.43 / 0.9275	30.33 / 0.841	29.09 / 0.8050	28.23 / 0.8535	33.65 / 0.9448
ISTAR (Ours)	<b>34.55 / 0.9284</b>	<b>30.48 / 0.8452</b>	<b>29.18 / 0.8076</b>	<b>28.56 / 0.8610</b>	<b>33.85 / 0.9467</b>	
$\times 4$	SRCNN [10]	30.48 / 0.8628	27.49 / 0.7503	26.90 / 0.7101	24.52 / 0.7221	27.66 / 0.8505
	FSRCNN [25]	30.71 / 0.8657	27.59 / 0.7535	26.98 / 0.7150	24.62 / 0.7280	27.90 / 0.8517
	VDSR [11]	31.35 / 0.8838	28.01 / 0.7674	27.29 / 0.7251	25.18 / 0.7524	28.83 / 0.8809
	DRCN [43]	31.53 / 0.8854	28.02 / 0.7670	27.23 / 0.7233	25.14 / 0.7510	28.98 / 0.8816
	CNF [44]	31.55 / 0.8856	28.15 / 0.7680	27.32 / 0.7253	-	-
	LapSRN [45]	31.54 / 0.8850	28.19 / 0.7720	27.32 / 0.7280	25.21 / 0.7560	29.09 / 0.8845
	DRRN [46]	31.68 / 0.8888	28.21 / 0.7720	27.38 / 0.7284	25.44 / 0.7638	29.46 / 0.8960
	BTSRN [47]	31.85 / -	28.20 / -	27.47 / -	25.74 / -	-
	MemNet [48]	31.74 / 0.8893	28.26 / 0.7723	27.40 / 0.7281	25.50 / 0.7630	29.42 / 0.8942
	SelNet [49]	32.00 / 0.8931	28.49 / 0.7783	27.44 / 0.7325	-	-
	SRDenseNet [58]	32.02 / 0.8934	28.50 / 0.7782	27.53 / 0.7337	26.05 / 0.7819	-
	CARN [50]	32.13 / 0.8937	28.60 / 0.7806	27.58 / 0.7349	26.07 / 0.7837	30.47 / 0.9084
	IMDN [15]	32.21 / 0.8948	28.58 / 0.7811	27.56 / 0.7353	26.04 / 0.7838	30.45 / 0.9075
	RAN [51]	31.43 / 0.8847	28.09 / 0.7691	27.31 / 0.7260	-	-
	DNCL [52]	31.66 / 0.8871	28.23 / 0.7717	27.39 / 0.7282	25.36 / 0.7606	-
	FilterNet [53]	31.74 / 0.8900	28.27 / 0.7730	27.39 / 0.7290	25.53 / 0.7680	-
	MRFN [54]	31.90 / 0.8916	28.31 / 0.7746	27.43 / 0.7309	25.46 / 0.7654	29.57 / 0.8962
	SeaNet-baseline [55]	32.18 / 0.8948	28.61 / 0.7822	27.57 / 0.7359	26.05 / 0.7896	30.44 / 0.9088
DEGREE [56]	31.47 / 0.8837	28.10 / 0.7669	27.20 / 0.7216	-	-	
Cross-SRN [57]	32.24 / 0.8954	28.59 / 0.7817	27.58 / 0.7364	26.16 / 0.7881	30.53 / 0.9081	
ISTAR (Ours)	<b>32.37 / 0.8972</b>	<b>28.74 / 0.7855</b>	<b>27.66 / 0.7391</b>	<b>26.38 / 0.7955</b>	<b>30.87 / 0.9130</b>	

DRRN [46], BTSRN [47], MemNet [48], SelNet [49], SRDenseNet [58], CARN [50], IMDN [15], RAN [51], DNCL [52], FilterNet [53], MRFN [54], SeaNet [55], DEGREE [56] and Cross-SRN [17]. Table IV shows the PSNR/SSIM comparisons on five testing benchmarks with scaling factor  $\times 2$ ,  $\times 3$  and  $\times 4$ .

In the figure, we can find that our ISTAR achieves the best

performance on all testing benchmarks with all scaling factors. Compared with Cross-SRN, our ISTAR achieves near 0.4 dB, 0.3 dB and 0.2 dB improvement on Urban100 dataset with scaling factor  $\times 2$ ,  $\times 3$  and  $\times 4$  separately. When scaling factor is  $\times 4$ , ISTAR achieves 0.34 dB PSNR higher than Cross-SRN on Manga109 dataset. It should be noticed that Urban100 and Manga109 are two representative datasets with plentiful edges

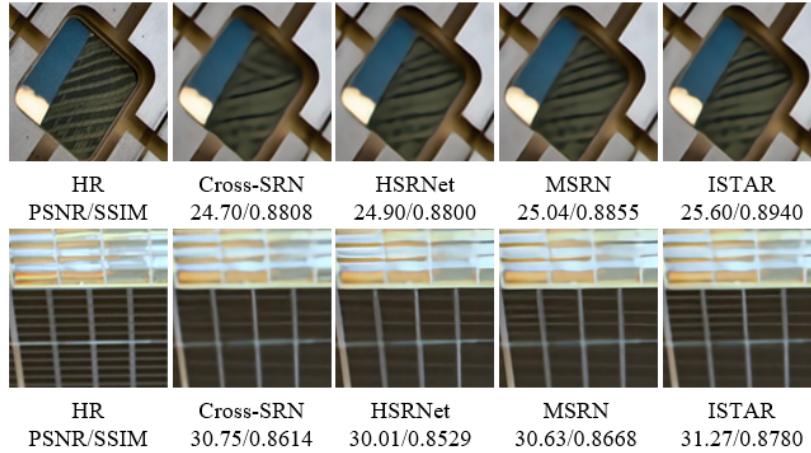


Fig. 7. Visualization comparisons on Urban100 dataset with scaling factor  $\times 4$

TABLE V  
PSNR/SSIM, PARAMETERS AND MACs COMPARISONS WITH  
OPTIMIZATION-INSPIRED NETWORKS WITH SCALING FACTOR  $\times 2$ .

Method	DBPN [59]	USRNet [21]	HSRNet [33]	ISTAR (Ours)
Param(M)	5.95	17.01	1.26	5.05
MACs(G)	3746.2	8545.8	808.2	1164.31
Set5	38.09 / 0.9600	37.76/0.9599	38.07 / 0.9607	38.15 / 0.9610
Set14	33.85 / 0.9190	33.43/0.9159	33.78 / 0.9197	33.79 / 0.9197
B100	32.27 / 0.9000	32.09/0.8985	32.26 / 0.9006	32.29 / 0.9010
Urban100	32.55 / 0.9324	31.78/0.9259	32.53 / 0.9320	32.65 / 0.9331

and lines. In this point of view, ISTAR can effectively restore the structural information than other works.

To further investigate the effectiveness of ISTAR, we compare the network with several optimization-inspired methods. Table V shows the PSNR/SSIM comparisons with different optimization-inspired networks. DBPN [59] is developed by the iterative back projection algorithm, while USRNet [21] and HSRNet [33] are inspired by the half-quadratic splitting (HQS) strategy. The MACs is calculated by the same method as the HSRNet. In the table, we can find that our ISTAR achieves better performance than USRNet and HSRNet. Compared with HSRNet, our method achieves 0.1 dB PSNR improvement on Set5 and Urban100 datasets. Furthermore, ISTAR achieves better performance than USRNet with near 29.7% parameters and 13.7% computation complexity. DBPN is one of the state-of-the-art image SR methods. Compared with DBPN, our method achieves competitive or better PSNR/SSIM results with similar parameters and 68.9% MACs off. In this point of view, ISTAR proves to be an effective optimization scheme for image SR.

Figure 7 shows the visualization comparisons with different recent image SR works (Cross-SRN [17], HSRNet [33] and MSRN [32]) on Urban100 dataset with scaling factor  $\times 4$ . In the first row of the figure, we can find that the building restored by ISTAR is closest to the ground-truth than other methods. Similarly, in the second row of the figure, ISTAR can restore the lines and grids more effectively than other works with much higher PSNR/SSIM results. In this point of view, ISTAR can generate more satisfying subjective results than other works.

## V. CONCLUSION

In this paper, we proposed an ISTA-inspired restoration network, termed ISTAR, for effective image super-resolution. We analyzed the image super-resolution task from the optimization perspective and proposed an iterative solution based on the ISTA. According to the formulation of the solution, an end-to-end network with optimization-inspired blocks was developed for effective image super-resolution. Multi-scale exploration and multi-scale attention mechanism were specifically devised to boost the network capacity. Experimental results show the proposed ISTAR achieves better subjective and objective performances than other state-of-the-art works. Compared with other optimization-inspired methods, ISTAR achieves competitive or better performance with much fewer parameters and lower computation complexity.

## REFERENCES

- [1] L. Zhang, H. Dai, and Y. Sang, "Med-srnet: Gan-based medical image super-resolution via high-resolution representation learning," *Computational Intelligence and Neuroscience*, vol. 2022, 2022.
- [2] S. Lei, H. Zijian, Y. Jiebin, and F. Fengchang, "Super resolution image visual quality assessment based on feature optimization," *Computational Intelligence and Neuroscience*, vol. 2022, 2022.
- [3] Y. Liu, X. Zhang, S. Wang, S. Ma, and W. Gao, "Spatial-temporal correlation learning for real-time video deinterlacing," in *2021 IEEE International Conference on Multimedia and Expo (ICME)*, 2021, pp. 1–6.
- [4] W. Gao, L. Tao, L. Zhou, D. Yang, X. Zhang, and Z. Guo, "Low-rate image compression with super-resolution learning," in *2020 IEEE/CVF Conference on Computer Vision and Pattern Recognition Workshops (CVPRW)*, 2020, pp. 607–610.
- [5] X. Tuo, Y. Xia, Y. Zhang, J. Zhu, Y. Zhang, Y. Huang, and J. Yang, "Super-resolution imaging for real aperture radar by two-dimensional deconvolution," in *2021 IEEE International Geoscience and Remote Sensing Symposium IGARSS*, 2021, pp. 6630–6633.
- [6] L. Li, T. Xu, and Y. Chen, "Fuzzy classification of high resolution remote sensing scenes using visual attention features," *Computational Intelligence and Neuroscience*, vol. 2017, 2017.
- [7] W. Wang, C. Zhang, J. Tian, X. Wang, J. Ou, J. Zhang, and J. Li, "High-resolution radar target recognition via inception-based vgg (ivgg) networks," *Computational Intelligence and Neuroscience*, vol. 2020, 2020.
- [8] J. Štastný and P. Sovka, "High-resolution movement eeg classification," *Computational intelligence and neuroscience*, vol. 2007, 2007.
- [9] Q. Ma, J. Jiang, X. Liu, and J. Ma, "Deep unfolding network for spatio-spectral image super-resolution," *IEEE Transactions on Computational Imaging*, vol. 8, pp. 28–40, 2022.

- [10] C. Dong, C. C. Loy, K. He, and X. Tang, "Image super-resolution using deep convolutional networks," *IEEE Transactions on Pattern Analysis and Machine Intelligence*, vol. 38, no. 2, pp. 295–307, 2016.
- [11] J. Kim, J. K. Lee, and K. M. Lee, "Accurate image super-resolution using very deep convolutional networks," in *2016 IEEE Conference on Computer Vision and Pattern Recognition (CVPR)*, 2016, pp. 1646–1654.
- [12] B. Lim, S. Son, H. Kim, S. Nah, and K. M. Lee, "Enhanced deep residual networks for single image super-resolution," in *2017 IEEE Conference on Computer Vision and Pattern Recognition Workshops (CVPRW)*, 2017, pp. 1132–1140.
- [13] Y. Zhang, Y. Tian, Y. Kong, B. Zhong, and Y. Fu, "Residual dense network for image restoration," *IEEE Transactions on Pattern Analysis and Machine Intelligence*, vol. 43, no. 7, pp. 2480–2495, 2021.
- [14] Y. Zhang, K. Li, K. Li, L. Wang, B. Zhong, and Y. Fu, "Image super-resolution using very deep residual channel attention networks," in *Computer Vision - ECCV 2018 - 15th European Conference, Munich, Germany, September 8-14, 2018, Proceedings, Part VII*, ser. Lecture Notes in Computer Science, V. Ferrari, M. Hebert, C. Sminchisescu, and Y. Weiss, Eds., vol. 11211. Springer, 2018, pp. 294–310. [Online]. Available: [https://doi.org/10.1007/978-3-030-01234-2\\_18](https://doi.org/10.1007/978-3-030-01234-2_18)
- [15] Z. Hui, X. Gao, Y. Yang, and X. Wang, "Lightweight image super-resolution with information multi-distillation network," in *ACM International Conference on Multimedia (MM)*, 2019, p. 2024–2032.
- [16] J. Liu, J. Tang, and G. Wu, "Residual feature distillation network for lightweight image super-resolution," in *Computer Vision - ECCV 2020 Workshops - Glasgow, UK, August 23-28, 2020, Proceedings, Part III*, ser. Lecture Notes in Computer Science, A. Bartoli and A. Fusiello, Eds., vol. 12537. Springer, 2020, pp. 41–55. [Online]. Available: [https://doi.org/10.1007/978-3-030-67070-2\\_2](https://doi.org/10.1007/978-3-030-67070-2_2)
- [17] Y. Liu, Q. Jia, X. Fan, S. Wang, S. Ma, and W. Gao, "Cross-srn: Structure-preserving super-resolution network with cross convolution," *IEEE Transactions on Circuits and Systems for Video Technology*, pp. 1–1, 2021.
- [18] K. Zhang, W. Zuo, S. Gu, and L. Zhang, "Learning deep CNN denoiser prior for image restoration," in *2017 IEEE Conference on Computer Vision and Pattern Recognition, CVPR 2017, Honolulu, HI, USA, July 21-26, 2017*. IEEE Computer Society, 2017, pp. 2808–2817. [Online]. Available: <https://doi.org/10.1109/CVPR.2017.300>
- [19] Y. Liu, S. Wang, J. Zhang, S. Wang, S. Ma, and W. Gao, "Iterative network for image super-resolution," *IEEE Transactions on Multimedia*, pp. 1–1, 2021.
- [20] K. Zhang, W. Zuo, and L. Zhang, "Deep plug-and-play super-resolution for arbitrary blur kernels," in *IEEE Conference on Computer Vision and Pattern Recognition, CVPR 2019, Long Beach, CA, USA, June 16-20, 2019*. Computer Vision Foundation / IEEE, 2019, pp. 1671–1681. [Online]. Available: [http://openaccess.thecvf.com/content\\_CVPR\\_2019/html/Zhang\\_Deep\\_Plug-And-Play\\_Super-Resolution\\_for\\_Arbitrary\\_Blur\\_Kernels\\_CVPR\\_2019\\_paper.html](http://openaccess.thecvf.com/content_CVPR_2019/html/Zhang_Deep_Plug-And-Play_Super-Resolution_for_Arbitrary_Blur_Kernels_CVPR_2019_paper.html)
- [21] K. Zhang, L. Van Gool, and R. Timofte, "Deep unfolding network for image super-resolution," in *2020 IEEE/CVF Conference on Computer Vision and Pattern Recognition (CVPR)*, 2020, pp. 3214–3223.
- [22] S. H. Chan, X. Wang, and O. A. Elgendy, "Plug-and-play admm for image restoration: Fixed-point convergence and applications," *IEEE Transactions on Computational Imaging*, vol. 3, no. 1, pp. 84–98, 2017.
- [23] Y. Yang, J. Sun, H. Li, and Z. Xu, "Deep admm-net for compressive sensing MRI," in *Advances in Neural Information Processing Systems 29: Annual Conference on Neural Information Processing Systems 2016, December 5-10, 2016, Barcelona, Spain*, D. D. Lee, M. Sugiyama, U. von Luxburg, I. Guyon, and R. Garnett, Eds., 2016, pp. 10–18. [Online]. Available: <https://proceedings.neurips.cc/paper/2016/hash/1679091c5a880faf6b5e6087eb1b2dc-Abstract.html>
- [24] Y. Wei, Y. Li, Z. Ding, Y. Wang, T. Zeng, and T. Long, "Sar parametric super-resolution image reconstruction methods based on admm and deep neural network," *IEEE Transactions on Geoscience and Remote Sensing*, vol. 59, no. 12, pp. 10197–10212, 2021.
- [25] C. Dong, C. C. Loy, and X. Tang, "Accelerating the super-resolution convolutional neural network," in *European Conference on Computer Vision*, B. Leibe, J. Matas, N. Sebe, and M. Welling, Eds., vol. 9906. Springer, 2016, pp. 391–407.
- [26] W. Shi, J. Caballero, F. Huszar, J. Totz, A. P. Aitken, R. Bishop, D. Rueckert, and Z. Wang, "Real-time single image and video super-resolution using an efficient sub-pixel convolutional neural network," in *IEEE Conference on Computer Vision and Pattern Recognition*. IEEE Computer Society, 2016, pp. 1874–1883.
- [27] K. He, X. Zhang, S. Ren, and J. Sun, "Deep residual learning for image recognition," in *2016 IEEE Conference on Computer Vision and Pattern Recognition (CVPR)*, 2016, pp. 770–778.
- [28] G. Huang, Z. Liu, L. van der Maaten, and K. Q. Weinberger, "Densely connected convolutional networks," in *2017 IEEE Conference on Computer Vision and Pattern Recognition, CVPR 2017, Honolulu, HI, USA, July 21-26, 2017*. IEEE Computer Society, 2017, pp. 2261–2269. [Online]. Available: <https://doi.org/10.1109/CVPR.2017.243>
- [29] J. Hu, L. Shen, and G. Sun, "Squeeze-and-excitation networks," in *2018 IEEE Conference on Computer Vision and Pattern Recognition, CVPR 2018, Salt Lake City, UT, USA, June 18-22, 2018*. Computer Vision Foundation / IEEE Computer Society, 2018, pp. 7132–7141. [Online]. Available: [http://openaccess.thecvf.com/content\\_cvpr\\_2018/html/Hu\\_Squeeze-and-Excitation\\_Networks\\_CVPR\\_2018\\_paper.html](http://openaccess.thecvf.com/content_cvpr_2018/html/Hu_Squeeze-and-Excitation_Networks_CVPR_2018_paper.html)
- [30] J. Liu, W. Zhang, Y. Tang, J. Tang, and G. Wu, "Residual feature aggregation network for image super-resolution," in *2020 IEEE/CVF Conference on Computer Vision and Pattern Recognition, CVPR 2020, Seattle, WA, USA, June 13-19, 2020*, pp. 2356–2365.
- [31] Y. Liu, X. Zhang, S. Wang, S. Ma, and W. Gao, "Sequential hierarchical learning with distribution transformation for image super-resolution," *ACM Trans. Multimedia Comput. Commun. Appl.*, apr 2022.
- [32] J. Li, F. Fang, K. Mei, and G. Zhang, "Multi-scale residual network for image super-resolution," in *European Conference on Computer Vision (ECCV)*, 2018, pp. 527–542.
- [33] Y. Liu, Q. Jia, J. Zhang, X. Fan, S. Wang, S. Ma, and W. Gao, "Hierarchical similarity learning for aliasing suppression image super-resolution," *CoRR*, vol. abs/2206.03361, 2022.
- [34] E. Agustsson and R. Timofte, "Ntire 2017 challenge on single image super-resolution: Dataset and study," in *IEEE Conference on Computer Vision and Pattern Recognition Workshops*, 2017, pp. 1122–1131.
- [35] M. Bevilacqua, A. Roumy, C. Guillemot, and M. line Alberi Morel, "Low-complexity single-image super-resolution based on nonnegative neighbor embedding," in *British Machine Vision Conference (BMVC)*, 2012, pp. 135.1–135.10.
- [36] R. Zeyde, M. Elad, and M. Protter, "On single image scale-up using sparse-representations," in *International Conference on Curves and Surfaces*. Springer, 2010, pp. 711–730.
- [37] D. Martin, C. Fowlkes, D. Tal, and J. Malik, "A database of human segmented natural images and its application to evaluating segmentation algorithms and measuring ecological statistics," in *IEEE International Conference on Computer Vision (ICCV)*, vol. 2, 2001, pp. 416–423 vol.2.
- [38] J. Huang, A. Singh, and N. Ahuja, "Single image super-resolution from transformed self-exemplars," in *IEEE Conference on Computer Vision and Pattern Recognition (CVPR)*, 2015, pp. 5197–5206.
- [39] Y. Matsui, K. Ito, Y. Aramaki, A. Fujimoto, T. Ogawa, T. Yamasaki, and K. Aizawa, "Sketch-based manga retrieval using manga109 dataset," *Multimedia Tools and Applications (MTA)*, vol. 76, no. 20, pp. 21811–21838, 2017.
- [40] D. P. Kingma and J. Ba, "Adam: A method for stochastic optimization," in *International Conference on Learning Representations*, 2015.
- [41] A. Horé and D. Ziou, "Image quality metrics: Psnr vs. ssim," in *International Conference on Pattern Recognition (ICPR)*, 2010, pp. 2366–2369.
- [42] Z. Wang, A. Bovik, H. Sheikh, and E. Simoncelli, "Image quality assessment: from error visibility to structural similarity," *IEEE Transactions on Image Processing*, vol. 13, no. 4, pp. 600–612, 2004.
- [43] J. Kim, J. K. Lee, and K. M. Lee, "Deeply-recursive convolutional network for image super-resolution," in *IEEE Conference on Computer Vision and Pattern Recognition*, 2016, pp. 1637–1645.
- [44] H. Ren, M. El-Khamy, and J. Lee, "Image super resolution based on fusing multiple convolution neural networks," in *IEEE Conference on Computer Vision and Pattern Recognition Workshops*, 2017, pp. 1050–1057.
- [45] W. Lai, J. Huang, N. Ahuja, and M. Yang, "Deep laplacian pyramid networks for fast and accurate super-resolution," in *IEEE Conference on Computer Vision and Pattern Recognition*, 2017, pp. 5835–5843.
- [46] Y. Tai, J. Yang, and X. Liu, "Image super-resolution via deep recursive residual network," in *IEEE Conference on Computer Vision and Pattern Recognition*, 2017, pp. 2790–2798.
- [47] Y. Fan, H. Shi, J. Yu, D. Liu, W. Han, H. Yu, Z. Wang, X. Wang, and T. S. Huang, "Balanced two-stage residual networks for image super-resolution," in *IEEE Conference on Computer Vision and Pattern Recognition Workshops*, 2017, pp. 1157–1164.
- [48] Y. Tai, J. Yang, X. Liu, and C. Xu, "Memnet: A persistent memory network for image restoration," in *IEEE International Conference on Computer Vision*, 2017, pp. 4549–4557.

- [49] J. Choi and M. Kim, "A deep convolutional neural network with selection units for super-resolution," in *2017 IEEE Conference on Computer Vision and Pattern Recognition Workshops*, 2017, pp. 1150–1156.
- [50] N. Ahn, B. Kang, and K. Sohn, "Fast, accurate, and lightweight super-resolution with cascading residual network," in *European Conference on Computer Vision*, vol. 11214, 2018, pp. 256–272.
- [51] Y. Wang, L. Wang, H. Wang, and P. Li, "Resolution-aware network for image super-resolution," *IEEE Transactions on Circuits and Systems for Video Technology*, vol. 29, no. 5, pp. 1259–1269, 2019.
- [52] C. Xie, W. Zeng, and X. Lu, "Fast single-image super-resolution via deep network with component learning," *IEEE Transactions on Circuits and Systems for Video Technology*, vol. 29, no. 12, pp. 3473–3486, 2019.
- [53] F. Li, H. Bai, and Y. Zhao, "Filternet: Adaptive information filtering network for accurate and fast image super-resolution," *IEEE Transactions on Circuits and Systems for Video Technology*, vol. 30, no. 6, pp. 1511–1523, 2020.
- [54] Z. He, Y. Cao, L. Du, B. Xu, J. Yang, Y. Cao, S. Tang, and Y. Zhuang, "MRFN: multi-receptive-field network for fast and accurate single image super-resolution," *IEEE Transactions on Multimedia*, vol. 22, no. 4, pp. 1042–1054, 2020.
- [55] F. Fang, J. Li, and T. Zeng, "Soft-edge assisted network for single image super-resolution," *IEEE Transactions on Image Processing*, vol. 29, pp. 4656–4668, 2020.
- [56] W. Yang, J. Feng, J. Yang, F. Zhao, J. Liu, Z. Guo, and S. Yan, "Deep edge guided recurrent residual learning for image super-resolution," *IEEE Transactions on Image Processing*, vol. 26, no. 12, pp. 5895–5907, 2017.
- [57] Y. Liu, Q. Jia, X. Fan, S. Wang, S. Ma, and W. Gao, "Cross-srn: Structure-preserving super-resolution network with cross convolution," *IEEE Transactions on Circuits and Systems for Video Technology*, pp. 1–1, 2021.
- [58] T. Tong, G. Li, X. Liu, and Q. Gao, "Image super-resolution using dense skip connections," in *IEEE International Conference on Computer Vision*. IEEE Computer Society, 2017, pp. 4809–4817.
- [59] M. Haris, G. Shakhnarovich, and N. Ukita, "Deep back-projection networks for single image super-resolution," *IEEE Transactions on Pattern Analysis and Machine Intelligence (TPAMI)*, pp. 1–1, 2020.